RSC Advances

PAPER

View Article Online
View Journal | View Issue

Cite this: *RSC Adv.*, 2024, **14**, 8108

Recycled PETg embedded with graphene, multi-walled carbon nanotubes and carbon black for high-performance conductive additive manufacturing feedstock†

Robert D. Crapnell, Elena Bernalte, Evelyn Sigley and Craig E. Banks *

The first report of conductive recycled polyethylene terephthalate glycol (rPETg) for additive manufacturing and electrochemical applications is reported herein. Graphene nanoplatelets (GNP), multi-walled carbon nanotubes (MWCNT) and carbon black (CB) were embedded within a recycled feedstock to produce a filament with lower resistance than commercially available conductive polylactic acid (PLA). In addition to electrical conductivity, the rPETg was able to hold >10 wt% more conductive filler without the use of a plasticiser, showed enhanced temperature stability, had a higher modulus, improved chemical resistance, lowered levels of solution ingress, and could be sterilised in ethanol. Using a mix of carbon materials CB/MWCNT/GNP (25/2.5/2.5 wt%) the electrochemical performance of the rPETg filament was significantly enhanced, providing a heterogenous electrochemical rate constant, k^0, equating to 0.88 (±0.01) × 10^{-3} cm s^{-1} compared to 0.46 (±0.02) × 10^{-3} cm s^{-1} for commercial conductive PLA. This work presents a paradigm shift within the use of additive manufacturing and electrochemistry, allowing the production of electrodes with enhanced electrical, chemical and mechanical properties, whilst improving the sustainability of the production through the use of recycled feedstock.

Received 13th December 2023
Accepted 22nd February 2024

DOI: 10.1039/d3ra08524d

rsc.li/rsc-advances

1. Introduction

Additive manufacturing, also commonly known as 3D-printing, is compiled of various manufacturing processes that utilise digital computer-aided design (CAD) files and processes them into 3D physical objects through the application of consecutive, layered cross-sections onto a build platform. It possesses significant benefits over its more traditional formative and subtractive manufacturing counterparts, such as: on-demand manufacturing, lower (often zero) waste, rapid prototyping capabilities, high degree of customisability, global reach as files can be modified and sent anywhere in the world, and the ability to create complex geometries such as nested and moving structures or overhangs.[1] Fused Filament Fabrication (FFF) is one type of additive manufacturing, which has seen widespread adoption due to the relatively low-cost of FFF printers and the simplicity of their use.[2] It involves the extrusion of a millimetre scale thermoplastic polymer filament through a heated nozzle. The movement of the print head draws the thin cross-section of polymer onto the previous, where it cools and solidifies to make the final 3D object. A wide range of commercial filaments are available for use on these printers, utilising different colours, polymers, and composites to produce a final object with the desired characteristics.

Polymer composite FFF filaments have become widely used in the production of additive manufacturing electrochemistry devices, primarily due to the low-cost of materials, ability to create lab equipment *in situ* and flexibility to produce a range of electrode geometries.[3] Although the range of commercially conductive FFF filaments is expanding,[4] the most widely utilised remains the carbon black/PLA composite, comprising of <21.43 wt% carbon black, >65 wt% PLA and <12.7 wt% unspecified polymer that acts as a plasticiser to improve the low-temperature. To produce an adequate electrochemical response the surface of the printed electrode is "activated" (essentially stripped of excess polymeric material), which has been achieved through various approaches with aqueous electrochemical activation in basic conditions being the most popular.[5] Combining conductive PLA and electrochemistry has been reported for a wide-range of applications, including general sensors,[6] biosensing platforms,[7] fuel cells and electrolysers,[8] batteries,[9] and supercapacitors.[10]

Recently researchers have been reporting the production of bespoke filaments, containing significantly higher loadings of conductive filler, and providing enhanced electrochemical performance.[11] Additionally, there has been reports of using

Faculty of Science and Engineering, Manchester Metropolitan University, Chester Street, M1 5GD, UK. E-mail: c.banks@mmu.ac.uk; Tel: +44(0)1612471196

† Electronic supplementary information (ESI) available. See DOI: https://doi.org/10.1039/d3ra08524d

recycled feedstock and bio-based plasticisers to improve the sustainability of additive manufacturing electrochemistry.[12]

The drive for improved sustainability stems from the inherent problems with using PLA, such as the poor chemical stability[13] and ingress of solutions,[14] effectively rendering additively manufactured electrodes single-use items. Poor chemical stability can be exacerbated though the use of additive manufacturing due to surface and microstructural defects produced by the printing process.[13] Although PLA is insoluble within the aqueous environments used in the electrochemistry field, the inherent permeability of PLA is particularly poor when compared to other common polymers. Solvent ingress like this results in polymer swelling,[15] which can lead to structural damage[16] and changes in the bulk mechanical[17] and electrical properties of the polymer.[14]

An alternative way to combat the issues with using PLA is to produce conductive filament from alternative thermoplastics, that still produce excellent printability whilst introducing enhanced chemical resistance. Polyethylene terephthalate glycol (PETg) is an example of a thermoplastic that delivers significant chemical resistance improvements when compared to PLA.[13,18] PETg offers resistance to water-miscible organic solvents, including the low molecular weight alcohols, potentially opening applications within the medical field as they can be sterilised with ethanol.[13] There has been reports in the literature for the production of carbon filled PETg, with the majority of this being carbon fibre filled for the purpose of improved mechanical properties.[19]

Herein, we report the development of the first electrically conductive PETg filament made from recycled feedstock through embedding different conductive carbon materials into the polymeric matrix. This work shows how additive manufacturing filaments can be made with enhanced physical and electrical properties, whilst being produced in a sustainable way.

2. Results and discussion

Recently researchers combining fused filament fabrication (FFF) additive manufacturing with electrochemistry have been reporting the production of bespoke filament that offers improved electrochemical performance when compared to the commonly used commercial conductive alternative.[10b,12c,12d] Utilising PLA or recycled PLA as the base polymer for the filaments allows for simple incorporation of conductive fillers, easy activation of additively manufactured electrodes through stripping of the surface PLA, and reproducible printing of parts in various geometries.[3a,12b] However, the use of PLA as a working electrode has always been single-shot due to the ingress of solution into the polymer matrix,[14] lack of simple surface regeneration methods, and the instability of the polymer in non-aqueous environments. To advance the field combining both FFF and electrochemistry, new conductive materials are required. In this work, we thoroughly report the fabrication and electrochemical application of the first conductive PETg made from recycled feedstocks.

2.1. Production and characterisation of functional recycled filament

All bespoke filaments in this work were produced through the recycling of old additive manufacturing (3D-printed) parts of polyethylene terephthalate glycol (PETg) filament. First, these prints were shredded to create fine granules and dried in a convection oven for a minimum of 2.5 h prior to use to remove any residual water ingressed into the polymer. Non-conductive recycled PETg (rPETg) filament was produced by simply passing the shredded prints through an extruder and collecting the filament. A scheme highlighting the production of conductive additive manufacturing filament from the rPETg is shown in Fig. 1A. Next, four different compositions of conductive rPETg were made using 70 wt% rPETg and 30 wt% total carbon/conductive filler. Specifically, the first composite used 30 wt% only carbon black (CB), the second used 25 wt% carbon black and 5 wt% multi-walled carbon nanotubes (MWCNT), the third used 25 wt% carbon black and 5 wt% graphene nanoplatelets (GNP), and the fourth used a combination of 25 wt% CB, 2.5 wt% MWCNT and 2.5 wt% GNP. In each case, the appropriate amounts of material were added to the chamber of a rheomixer set to 230 °C and mixed using Banbury rotors for 5 min at 70 rpm. Once mixed, the material was extracted from the machine and allowed to cool to room temperature before being shredded. The composite was then passed through an extruder to produce the electrically conductive filaments. Interestingly, most reports of PLA with high conductive filler loading require the addition of a plasticiser to ensure adequate low-temperature flexibility for additive manufacturing (3D-printing).[10b,12d] In the case of PETg, all conductive filaments produced showed high flexibility without any additional plasticiser compound, as shown in Fig. 1B.

To initially investigate the suitability of our bespoke conductive rPETg filaments compared to the commercially available PLA, which has been utilised throughout the literature,[3b,3c,6a,20] we first measured the resistance across 10 cm of filament. The commercial conductive PLA has a quoted resistance from their manufacturer of between 2 and 3 kΩ over a 10 cm length of their 1.75 mm filament.[21] However, using a standard digital multi-meter, the resistance measured across the commercial filament was 1.31 ± 0.03 kΩ over multiple measurements ($N = 6$). On the other hand, following the same procedure for our bespoke filaments, we observed that the 30 wt% CB rPETg filament did not produce a 10 cm resistance reading, indicating no conductivity was present and this filament was therefore not tested further throughout this work. The CB/MWCNT (25/5 wt%) filament produced a measurement of 3.45 ± 0.27 kΩ, the CB/GNP (25/5 wt%) filament produced a reading of 1.50 ± 0.13 kΩ, and the CB/MWCNT/GNP (25/2.5/2.5 wt%) filament produced a reading of 0.71 ± 0.03 kΩ. This indicated that the mixed material filaments produced significantly better conductivity throughout the polymer matrix, and with all three carbon materials embedded in the rPETg filament the conductivity is better than the commercially available PLA filaments, alongside other benefits inherent from the plastic physicochemical properties.

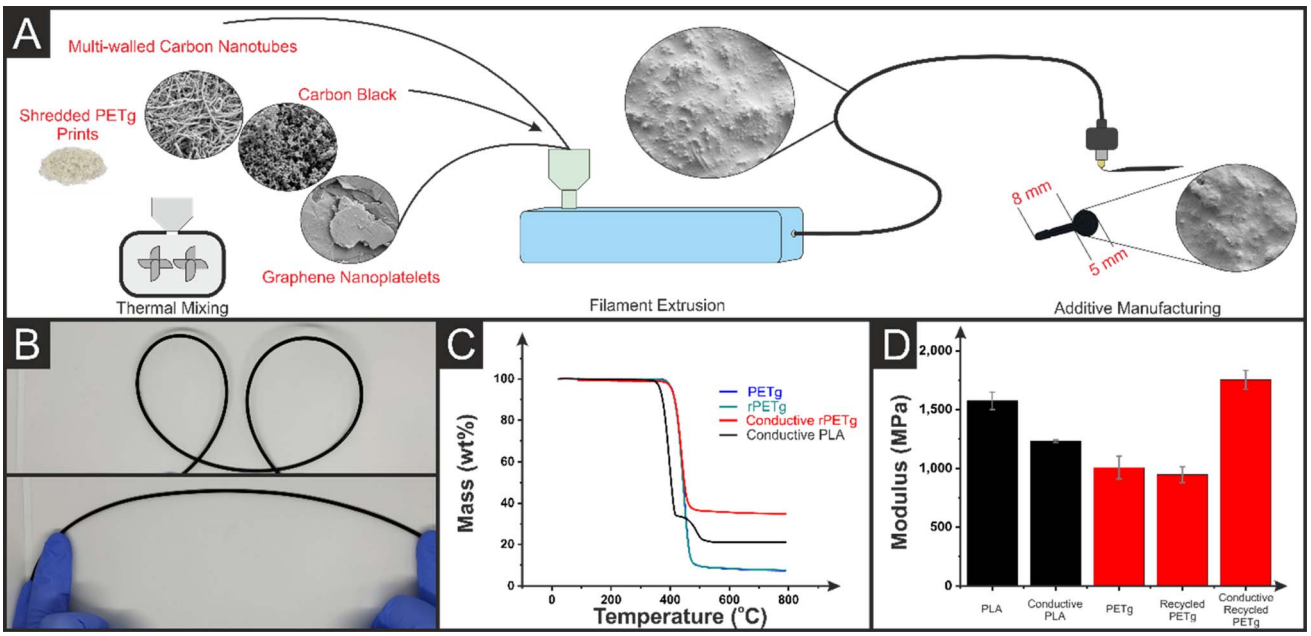

Fig. 1 (A) Schematic for the production of conductive recycled PETg additive manufacturing filament. (B) Photographs highlighting the flexibility of the conductive rPETg filament. (C) Thermogravimetric analysis of the conductive rPETg (25 wt% CB, 2.5 wt% GNP, 2.5 wt% MWCNT). (D) Plot of the modulus obtained from tensile testing, with error calculated from three repeat samples.

Thermogravimetric analysis was performed on the CB/MWCNT/GNP (25/2.5/2.5 wt%), Fig. 1C, to investigate the temperature stability of the filament in comparison to the original PETg filament used for previous prints, rPETg with no fillers, and commercial conductive PLA filament. It is important to analyse the original feedstocks to understand whether historical processing or the subsequent thermal treatments from producing the bespoke filament affect the stability of the polymer. Additionally, through analysis of the final mass of the filaments after the polymer degradation, accurate information about the mass of conductive filler within the final filament can be calculated. A summary of the data obtained from TGA analysis can be found in Table 1, where it is clear that all PETg based filaments have a higher onset of degradation temperature than the PLA filaments, indicating enhanced thermal stability. The bespoke CB/MWCNT/GNP (25/2.5/2.5 wt%) filament recorded an onset temperature of 348 ± 1 °C compared to 304 ± 2 °C for the commercially conductive PLA and 283 ± 3 °C for previously reported conductive recycled PLA.[12a] Moreover, there is a reduction of ~20 °C in onset temperature between the non-conductive PETg filaments and the CB/MWCNT/GNP (25/2.5/2.5 wt%). As the rPETg did not show this large reduction in onset temperature compared to the initial PETg, it is expected to be due to the additional thermal mixing process required to combine the carbon materials with the polymer. Both non-conductive PETg filaments had final weights of ~7 wt%, this was therefore subtracted from the final weight of the CB/MWCNT/GNP (25/2.5/2.5 wt%) filament to obtain the mass due solely to the conductive fillers, giving a value of 28 ± 3 wt%.

Next, the mechanical properties of the CB/MWCNT/GNP (25/2.5/2.5 wt%) were tested against the same filaments as above, through the production of AM tensile testing specimen (Type IV, ASTM D638). The modulus ($N = 3$) for each filament, Fig. 1D, was calculated from their respective stress–strain plots, Fig. S1,† and is summarised in Table 1. Interestingly the non-conductive PETg used throughout this work gave lower modulus results when compared to PLA, however when the carbon nanomaterials were added to the rPETg matrix a large increase was

Table 1 Thermal and mechanical properties of the original PETg, recycled PETg, conductive rPETg, commercial PLA and commercial conductive PLA. Summarising the degradation onset temperature, final mass, conductive filler content and the modulus. The uncertainties are the standard deviations of three repeat measurements

Filament	Onset T (°C)	Final mass (wt%)	Filler content (wt%)	Modulus (MPa)
PETg	371 ± 3	7 ± 1	—	1008 ± 97
rPETg	365 ± 5	7 ± 2	—	948 ± 68
CB/MWCNT/GNP rPETg	348 ± 1	35 ± 1	28 ± 3	1753 ± 83
PLA	306 ± 4	—	—	1574 ± 75
CB PLA	304 ± 2	20 ± 4	20 ± 4	1231 ± 12

observed. Without the conductive filler, the rPETg produced a modulus of 948 ± 68 MPa, compared to 1753 ± 83 MPa with the CB/MWCNT/GNP embedded. Such and improvement in the modulus of plastic composites after adding these nanomaterials is attributed to their high intrinsic mechanical properties.[22] This value was also significantly higher than the commercial CB PLA, indicating that the produced conductive rPETg filament possessed an improved mechanical strength to add to its improved thermal stability.

2.2. Physicochemical characterisation of additively manufactured electrodes

As we demonstrated above, the CB/MWCNT/GNP rPETg filament produced the lowest resistance across the filament. This filament was then utilised to print additive manufactured electrodes, which could be used for electrochemical characterisation. Throughout the literature, additively manufactured electrodes have been "activated" to improve their electrochemical performance, by removing excess of non-conductive polymeric material from the surface of the print, revealing increased proportions of conductive filler.[5a] Such electrochemical activation is typically carried out by applying chronoamperometry in NaOH (0.5 M). Activation profiles for the CB/MWCNT/GNP rPETg and the commercial conductive PLA are presented in Fig. 2A. Although similar profiles are observed in both cases, an increase in current values is shown by the conductive rPETg that indicates an improvement in the additively manufactured electrodes ability to perform electrochemical experiments. The activation profiles for the CB/GNP (25/5 wt%) and CB/MWCNT (25/5 wt%) filaments can be found in Fig. S2.†

To investigate the surface chemical composition of the rPETg additively manufactured electrodes and confirm successful activation, XPS analysis was performed. Fig. 2B and C shows the C 1s and O 1s spectrum of the activated CB/MWCNT/GNP (25/2.5/2.5 wt%) filament, whilst the non-activated spectrum can be found in Fig. S3.† It can be seen that there are three symmetric peaks fitted, identified as C–C/C–H bonding, C–O bonding, and O–C=O bonding, with the C–C/C–H bonding peak of approximately 4 times the intensity of the other two. Additionally, an asymmetric peak at 284.5 eV was required, consistent with the X-ray photoelectron emission by graphitic carbon, alongside a symmetric peak at ~291 eV assigned to the π–π* transitions seen within graphitic carbon.[23] Upon electrochemical activation of the rPETg AME, there is an increase in the atomic concentration of the graphitic peak from 5.5% to 9.0%, indicating the successful activation of the AME. Interestingly, for previous reports on bespoke conductive PLA filaments, there is often a larger increase in the intensity of the graphitic peaks upon electrochemical activation[10b,12b–d] than the observed here for the bespoke rPETg, which indicates that this activation procedure is less effective for PETg due to the stronger chemical resistance of the polymer.[13]

Raman analysis was performed on the activated CB/MWCNT/GNP (25/2.5/2.5 wt%) AME, Fig. 2D, showing the characteristic intense peaks at 1338, 1572 and 2680 cm^{-1}, which

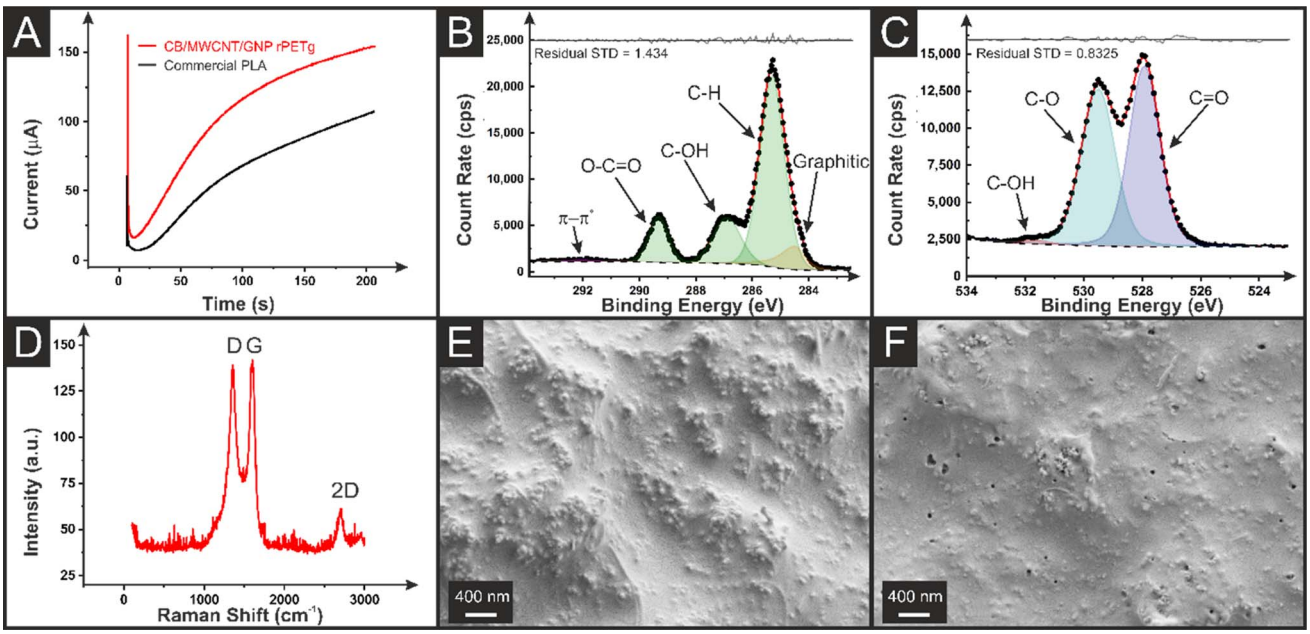

Fig. 2 (A) Electrochemical activation profiles for the rPETg (25 wt% CB, 2.5 wt% GNP, 2.5 wt% MWCNT) and commercial conductive PLA. Activated using chronoamperometry in NaOH (0.5 M) at +1.4 V for 200 s and −1.0 V for 200 s. Performed using a nichrome wire counter electrode and Ag|AgCl reference electrode (3 M KCl). (B) The XPS C 1s region for the rPETg (25 wt% CB, 2.5 wt% GNP, 2.5 wt% MWCNT) after electrochemical activation. (C) The XPS O 1s region for the rPETg (25 wt% CB, 2.5 wt% GNP, 2.5 wt% MWCNT) after electrochemical activation. (D) Raman spectra for rPETg (25 wt% CB, 2.5 wt% GNP, 2.5 wt% MWCNT) after electrochemical activation. (E) SEM image of the rPETg (25 wt% CB, 2.5 wt% GNP, 2.5 wt% MWCNT) electrode surface before electrochemical activation. (F) SEM image of the rPETg (25 wt% CB, 2.5 wt% GNP, 2.5 wt% MWCNT) after electrochemical activation.

are assigned to the D-, G-, and 2D-bands of graphitic-like structures, with an ID/IG ratio calculated to be 1.00.[24] The presence of these carbon materials on the surface of the additive manufactured electrodes is also confirmed through SEM images before and after activation, Fig. 2E and F respectively. The SEM images show the presence of the different conductive fillers used, including the spheres of carbon black, sheets of graphene and cylinders of MWCNTs, these morphologies cannot be seen on the surface of non-filled PETg, Fig. S4.† It can be seen that even on the electrochemically activated sample there is a large covering of polymeric material, providing more evidence toward the improved chemical stability of the rPETg filament in basic conditions when compared to previous reports involving PLA.[10b,12b–d] In the micrograph of the activated AME, Fig. 2F, there are also some clear perforations in the polymer surface supporting the observations extracted from XPS analysis indicating that there would be an enhanced amount of graphitic carbon available and hence a better performance towards electrochemical applications.

The physicochemical characterisation of the additively manufactured electrodes printed from CB/MWCNT/GNP (25/2.5/2.5 wt%) provides substantial evidence that the CB/MWCNT/GNP (25/2.5/2.5 wt%) rPETg filament offers enhanced chemical stability toward alkaline conditions in the same way non-conductive PETg offers improved chemical stability over non-conductive PLA.[13]

2.3. Electrochemical characterisation

Electrochemical characterisation of the additively manufactured electrodes printed from the three conductive rPETg filaments was performed against common outer- and inner-sphere redox probes hexaammineruthenium(III) chloride $[Ru(NH_3)_6]^{3+}$ and $[Fe(CN)_6]^{4-/3-}$ and additionally benchmarked *versus* additive manufactured electrodes printed with commercially available conductive PLA filament. The use of scan rate studies in $[Ru(NH_3)_6]^{3+}$ allows for the best determination of the heterogeneous electrochemical rate constant (k^0) and the real electrochemical surface area (A_e)[25] Fig. 3A presents an example of the scan rate study obtained for the CB/MWCNT/GNP (25/2.5/2.5 wt%) additive manufactured electrode against the near-ideal outer sphere redox probe $[Ru(NH_3)_6]^{3+}$ (1 mM in 0.1 M KCl), showing the classical redox peaks for the one-electron reduction and oxidation. Fig. 3B shows a comparison between the three bespoke conductive rPETg filaments using cyclic voltammetry (25 mV s^{-1}) against $[Ru(NH_3)_6]^{3+}$ (1 mM in 0.1 M KCl), where a clear improvement in peak currents and peak-to-peak separation (ΔE_p) can be seen for the CB/MWCNT/GNP (25/2.5/2.5 wt%) additively manufactured electrode. A summary of the data obtained from the electrochemical studies in this work is presented in Table 2. From inspection of Table 2 it can be seen that the additive manufactured electrode printed from the CB/MWCNT/GNP (25/2.5/2.5 wt%) rPETg filament produced the best k^0 value of $(0.88 \pm 0.01) \times 10^{-3}$ cm s^{-1}, improving significantly compared to the other rPETg filaments tested and the commercial conductive PLA, which produced a value of $(0.46 \pm 0.02) \times 10^{-3}$ cm s^{-1}. This highlights the excellent performance of the CB/MWCNT/GNP (25/2.5/2.5 wt%) rPETg filament toward outer-sphere probes and is consistent with the resistance values measured previously.

It is important to understand the electrochemical performance of the CB/MWCNT/GNP (25/2.5/2.5 wt%) rPETg filament against inner-sphere probes such as $[Fe(CN)_6]^{4-/3-}$, since it is necessary to activate the electrodes beforehand. It was seen in the XPS and SEM results that less surface polymer was removed from the rPETg filament in comparison to the commercial conductive PLA after activation, which could hinder the performance against this type of probe. Fig. 3C presents the Nyquist plots obtained through electrochemical impedance spectroscopy (EIS) in $[Fe(CN)_6]^{4-/3-}$ (0.1 M KCl) for both additively manufactured electrodes printed from the CB/MWCNT/GNP (25/2.5/2.5 wt%) rPETg filament and the commercial conductive PLA. It is demonstrated from Fig. 3C and Table 2 that both systems produced similar charge-transfer resistances (R_{CT}) but interestingly, a significant improvement in solution resistance (R_S) for the CB/MWCNT/GNP (25/2.5/2.5 wt%) rPETg additively manufactured electrode. This indicates that the resistance introduced into the system by the additively manufactured electrode is lower for the rPETg electrode at 0.35 ± 0.01 kΩ compared to 0.78 ± 0.01 kΩ for the commercial PLA. Even so, the comparable R_{CT} values indicates that the NaOH activation does not expose enough carbon due to excellent PETg chemical stability in this media. Even greater performance could be achieved for the rPETg through a different activation procedure that revealed increased amounts of conductive filler such as mechanical, plasma, or alternative chemical activation. Similar indications are seen in Fig. 3D, showing the CV (50 mV s^{-1}) profile in $[Fe(CN)_6]^{4-/3-}$ (0.1 M KCl) of the CB/MWCNT/GNP (25/2.5/2.5 wt%) rPETg additively manufactured electrode and commercial conductive PLA additively manufactured electrode. It can be seen that there is a small improvement in peak current and ΔE_p, showing that the rPETg filament outperforms the PLA electrochemically, even whilst not effectively activated due to the intrinsic stability of the polymer.

As mentioned previously, a common issue with the use of conductive PLA for the production of additively manufactured electrodes is the ingress of solution into the polymeric matrix, rendering the electrode ineffective after a single use.[14] Fig. 3E shows cyclic voltammetric (50 mV s^{-1}) profiles for additively manufactured electrodes in electrolyte only containing 0.1 M KCl after they have been systematically cycled in $[Ru(NH_3)_6]^{3+}$ (1 mM in 0.1 M KCl) and washed with deionised water. It is demonstrated that there is a significantly lower cyclic voltammetric response using the conductive rPETg, indicating that these additively manufactured electrodes are more resistant to experience ingressing of $[Ru(NH_3)_6]^{3+}$ into the electrode or adsorbed onto the surface. This shows that the rPETg electrode could be used multiple times with the right cleaning methodology developed, which would greatly reduce the environmental impact of using single-shot additively manufactured electrodes.

One important application of additively manufactured and electrochemistry is the development of point-of-care devices,[12c,26] where sterilisation of the sensing platforms is of vital importance to reduce the risk of transmitting infections. Fig. 3F

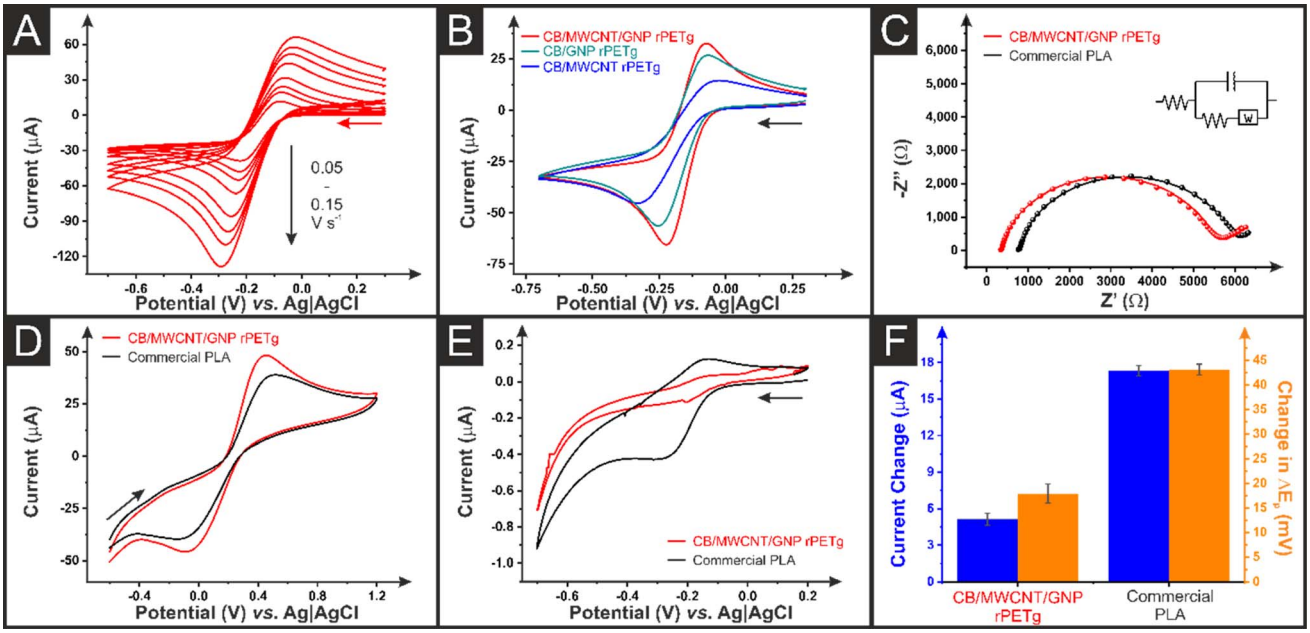

Fig. 3 (A) Scan rate study (5–150 mV s^{-1}) in $[Ru(NH_3)_6]^{3+}$ (1 mM in 0.1 M KCl) performed with the rPETg (25 wt% CB, 2.5 wt% GNP, 2.5 wt% MWCNT) additive manufactured electrodes as the WE, nichrome coil CE, and Ag|AgCl as RE. (B) Cyclic voltammograms (25 mV s^{-1}) in $[Ru(NH_3)_6]^{3+}$ (1 mM in 0.1 M KCl) performed with the rPETg (25 wt% CB, 2.5 wt% GNP, 2.5 wt% MWCNT), (25 wt% CB, 5 wt% GNP), and (25 wt% CB, 5 wt% MWCNT) additive manufactured electrodes as the WE, nichrome coil CE, and Ag|AgCl as RE. (C) EIS Nyquist plots comparing rPETg (25 wt% CB, 2.5 wt% GNP, 2.5 wt% MWCNT) with commercial PLA additive manufactured electrodes as the WE. Performed in $[Fe(CN)_6]^{4-/3-}$ (1 mM in 0.1 M KCl) with a nichrome coil CE, and Ag|AgCl as RE. (D) Cyclic voltammograms (50 mV s^{-1}) comparing rPETg (25 wt% CB, 2.5 wt% GNP, 2.5 wt% MWCNT) with commercial PLA additive manufactured electrodes as the WE. Performed in $[Fe(CN)_6]^{4-/3-}$ (1 mM in 0.1 M KCl) with a nichrome coil CE, and Ag|AgCl as RE. (E) Cyclic voltammograms (50 mV s^{-1}) comparing rPETg (25 wt% CB, 2.5 wt% GNP, 2.5 wt% MWCNT) with commercial PLA additive manufactured electrodes as the WE after being previously used in $[Ru(NH_3)_6]^{3+}$ (1 mM in 0.1 M KCl) and washed with deionised water. Performed in 0.1 M KCl with a nichrome coil CE, and Ag|AgCl as RE. (F) Plot showing the change in peak current and peak-to-peak separation for additive manufactured electrodes printed from rPETg (25 wt% CB, 2.5 wt% GNP, 2.5 wt% MWCNT) and commercial PLA after being sonicated in ethanol (70%) for 10 min. Calculations based on cyclic voltammograms (50 mV s^{-1}) comparing rPETg (25 wt% CB, 2.5 wt% GNP, 2.5 wt% MWCNT) with commercial PLA additive manufactured electrodes as the WE in $[Ru(NH_3)_6]^{3+}$ (1 mM in 0.1 M KCl) with a nichrome coil CE, and Ag|AgCl as RE.

represents the changes in cyclic voltammetric profile (50 mV s^{-1}) for the $[Ru(NH_3)_6]^{3+}$ peak currents and ΔE_p before and after sonication of conductive rPETg additive manufactured electrode for 10 min within a 70% ethanol solution as standard sterilisation product. For the rPETg additive manufactured electrode, it can be seen that there is only a small change in the peak current after sonication, corresponding to an RSD = 6.0%, which falls in line with natural variation between many additively manufactured electrode sensors.[27] This is compared to the conductive commercial PLA which exhibited an RSD = 21.3%. For the change in ΔE_p, the rPETg electrode produced a shift of only 17 ± 2 mV compared to 43 ± 2 mV for the commercial conductive PLA, highlighting the improved chemical stability of the rPETg filament and the possibility of it to be sterilised prior to use.

The improved electrochemical properties of the CB/MWCNT/GNP (25/2.5/2.5 wt%) rPETg, alongside the improved chemical, mechanical and thermal properties, highlights how the use of filaments from this material could revolutionise the combination of additive manufacturing electrodes and electrochemistry.

Table 2 Comparisons of the heterogeneous electron transfer (k^0), electrochemically active area (A_e), EIS charge transfer resistance (R_{ct}) and solution resistance (R_s) for the commercial conductive PLA and the three bespoke rPETg filaments. The uncertainties are the standard deviations across three different additive manufactured electrode measurements

Filament	k^0 ($\times 10^{-3}$ cm s^{-1})	A_e (cm^2)	R_S (kΩ)	R_{CT} (kΩ)
CB/MWCNT PETg	0.20 ± 0.04	0.32 ± 0.03	0.89 ± 0.02	21.4 ± 0.18
CB/GNP PETg	0.53 ± 0.02	0.43 ± 0.03	0.73 ± 0.01	8.81 ± 0.08
CB/MWCNT/GNP rPETg	0.88 ± 0.01	0.48 ± 0.02	0.35 ± 0.01	5.11 ± 0.04
Commercial PLA	0.46 ± 0.02	0.54 ± 0.02	0.78 ± 0.01	5.19 ± 0.04

3. Conclusions

In this work we have presented the production of the first electrically conductive PETg filament, made from recycled PETg prints embedded with graphene nanoplatelets, multi-walled carbon nanotubes and carbon black. The rPETg filament was able to be fabricated without the addition of a plasticiser, whilst still maintaining excellent low-temperature flexibility. The rPETg filament had an improved temperature stability, chemical resistance and modulus compared to that of the commercially conductive PLA filament used regularly throughout the literature. Electrochemical characterisation of additively manufactured electrodes printed from the rPETg filament highlighted that a combination of all the carbon materials produced a filament with improved conductivity. The CB/MWCNT/GNP (25/2.5/2.5 wt%) rPETg filament showed a significantly improved k^0 compared to the commercially conductive PLA, emphasising the improved electrochemical performance in addition to its other beneficial characteristics. The rPETg additively manufactured electrodes showed significantly less ingress of solution, indicating that it could be used more than a single-shot electrode. Additionally, sterilisation in ethanol translated in minimal changes in the electrochemical response, opening the possibility for future use in healthcare settings. This work presents a paradigm shift in how additive manufacturing and electrochemistry can be combined to produce high quality electrodes from different materials, whilst still utilising recycled feedstock to further improve the sustainability of the field.

Conflicts of interest

The authors declare no conflict of interest.

Acknowledgements

We thank EPSRC for funding (EP/W033224/1).

References

1 M. Attaran, *Bus. Horiz.*, 2017, **60**, 677.
2 S. C. Ligon, R. Liska, J. Stampfl, M. Gurr and R. Mülhaupt, *Chem. Rev.*, 2017, **117**, 10212.
3 (*a*) A. G.-M. Ferrari, N. J. Hurst, E. Bernalte, R. D. Crapnell, M. J. Whittingham, D. A. Brownson and C. E. Banks, *Analyst*, 2022, **147**, 5121; (*b*) M. J. Whittingham, R. D. Crapnell, E. J. Rothwell, N. J. Hurst and C. E. Banks, *Talanta Open*, 2021, **4**, 100051; (*c*) M. J. Whittingham, R. D. Crapnell and C. E. Banks, *Anal. Chem.*, 2022, **94**, 13540.
4 K. K. Hussain, R. S. Shergill, H. H. Hamzah, M. S. Yeoman and B. A. Patel, *ACS Appl. Polym. Mater.*, 2023, **5**, 4136.
5 (*a*) E. M. Richter, D. P. Rocha, R. M. Cardoso, E. M. Keefe, C. W. Foster, R. A. Munoz and C. E. Banks, *Anal. Chem.*, 2019, **91**, 12844; (*b*) D. P. Rocha, R. G. Rocha, S. V. Castro, M. A. Trindade, R. A. Munoz, E. M. Richter and L. Angnes, *Electrochem. Sci. Adv.*, 2022, **2**, e2100136.
6 (*a*) R. D. Crapnell, E. Bernalte, A. G.-M. Ferrari, M. J. Whittingham, R. J. Williams, N. J. Hurst and C. E. Banks, *ACS Meas. Sci. Au*, 2021, **2**, 167; (*b*) A. Abdalla and B. A. Patel, *Annu. Rev. Anal. Chem.*, 2021, **14**, 47; (*c*) A. Abdalla and B. A. Patel, *Curr. Opin. Electrochem.*, 2020, **20**, 78; (*d*) R. M. Cardoso, C. Kalinke, R. G. Rocha, P. L. Dos Santos, D. P. Rocha, P. R. Oliveira, B. C. Janegitz, J. A. Bonacin, E. M. Richter and R. A. Munoz, *Anal. Chim. Acta*, 2020, **1118**, 73.
7 (*a*) J. Muñoz and M. Pumera, *TrAC, Trends Anal. Chem.*, 2020, **128**, 115933; (*b*) M. Pumera, *Curr. Opin. Electrochem.*, 2019, **14**, 133; (*c*) L. R. Silva, A. Gevaerd, L. H. Marcolino-Junior, M. F. Bergamini, T. A. Silva and B. C. Janegitz, in *Advances in Bioelectrochemistry Volume 2: Biomimetic, Bioelectrocatalysis and Materials Interfaces*, Springer, 2022.
8 (*a*) P. L. dos Santos, S. J. Rowley-Neale, A. G. M. Ferrari, J. A. Bonacin and C. E. Banks, *ChemElectroChem*, 2019, **6**, 5633; (*b*) J. P. Hughes, P. L. dos Santos, M. P. Down, C. W. Foster, J. A. Bonacin, E. M. Keefe, S. J. Rowley-Neale and C. E. Banks, *Sustainable Energy Fuels*, 2020, **4**, 302.
9 (*a*) C. W. Foster, G. Q. Zou, Y. Jiang, M. P. Down, C. M. Liauw, A. Garcia-Miranda Ferrari, X. Ji, G. C. Smith, P. J. Kelly and C. E. Banks, *Batteries Supercaps*, 2019, **2**, 448; (*b*) X. Gao, M. Zheng, X. Yang, R. Sun, J. Zhang and X. Sun, *Mater. Today*, 2022, **59**, 161.
10 (*a*) M. Li, S. Zhou, L. Cheng, F. Mo, L. Chen, S. Yu and J. Wei, *Adv. Funct. Mater.*, 2023, **33**, 2208034; (*b*) P. Wuamprakhon, R. D. Crapnell, E. Sigley, N. J. Hurst, R. J. Williams, M. Sawangphruk, E. M. Keefe and C. E. Banks, *Adv. Sustainable Syst.*, 2023, **7**, 2200407; (*c*) C. W. Foster, M. P. Down, Y. Zhang, X. Ji, S. J. Rowley-Neale, G. C. Smith, P. J. Kelly and C. E. Banks, *Sci. Rep.*, 2017, **7**, 42233; (*d*) A. García-Miranda Ferrari, J. L. Pimlott, M. P. Down, S. J. Rowley-Neale and C. E. Banks, *Adv. Energy Mater.*, 2021, **11**, 2100433.
11 (*a*) L. R. G. Silva, J. S. Stefano, R. C. F. Nocelli and B. C. Janegitz, *Food Chem.*, 2023, **406**, 135038; (*b*) K. Ghosh, S. Ng, C. Iffelsberger and M. Pumera, *Appl. Mater. Today*, 2022, **26**, 101301; (*c*) C. Iffelsberger, C. W. Jellett and M. Pumera, *Small*, 2021, **17**, 2101233.
12 (*a*) R. D. Crapnell, I. V. Arantes, M. J. Whittingham, E. Sigley, C. Kalinke, B. C. Janegitz, J. A. Bonacin, T. R. Paixão and C. E. Banks, *Green Chem.*, 2023, **25**, 5591; (*b*) R. D. Crapnell, E. Sigley, R. J. Williams, T. Brine, A. Garcia-Miranda Ferrari, C. Kalinke, B. C. Janegitz, J. A. Bonacin and C. E. Banks, *ACS Sustain. Chem. Eng.*, 2023, **11**(24), 9183; (*c*) C. Kalinke, R. D. Crapnell, E. Sigley, M. J. Whittingham, P. R. de Oliveira, L. C. Brazaca, B. C. Janegitz, J. A. Bonacin and C. E. Banks, *Chem. Eng. J.*, 2023, 143513; (*d*) E. Sigley, C. Kalinke, R. D. Crapnell, M. J. Whittingham, R. J. Williams, E. M. Keefe, B. C. Janegitz, J. A. Bonacin and C. E. Banks, *ACS Sustain. Chem. Eng.*, 2023, **11**, 2978.
13 K. S. Erokhin, E. G. Gordeev and V. P. Ananikov, *Sci. Rep.*, 2019, **9**, 1.
14 R. J. Williams, T. Brine, R. D. Crapnell, A. G.-M. Ferrari and C. E. Banks, *Mater. Adv.*, 2022, **3**, 7632.

15 U. Sonchaeng, F. Iniguez-Franco, R. Auras, S. Selke, M. Rubino and L.-T. Lim, *Prog. Polym. Sci.*, 2018, **86**, 85.
16 V. Kefalas, *J. Appl. Polym. Sci.*, 1995, **58**, 711.
17 K. Loos, V. M. Bruère, B. Demmel, Y. Ilmberger, A. Lion and M. Johlitz, *Polymers*, 2021, **13**, 4402.
18 D. Moreno Nieto, M. Alonso-García, M.-A. Pardo-Vicente and L. Rodríguez-Parada, *Polymers*, 2021, **13**, 1036.
19 (*a*) I. M. Alarifi, *Polym. Test.*, 2023, **120**, 107949; (*b*) E. García, P. Núñez, M. Caminero, J. Chacón and S. Kamarthi, *Composites, Part B*, 2022, **235**, 109766; (*c*) D. Jiang and D. E. Smith, *Addit. Manuf.*, 2017, **18**, 84; (*d*) S. Kasmi, G. Ginoux, S. Allaoui and S. Alix, *J. Appl. Polym. Sci.*, 2021, **138**, 50955.
20 H. M. Elbardisy, E. M. Richter, R. D. Crapnell, M. P. Down, P. G. Gough, T. S. Belal, W. Talaat, H. G. Daabees and C. E. Banks, *Anal. Methods*, 2020, **12**, 2152.
21 Proto-pasta, Proto Plant, 2022, **https://cdn.shopify.com/s/files/1/0717/9095/files/CDP1xxxx_SDS.pdf?1992606272897634343**.
22 (*a*) N. Viet, Q. Wang and W. Kuo, *Composites, Part B*, 2016, **94**, 160; (*b*) J. Wang, F. Song, Y. Ding and M. Shao, *Mater. Des.*, 2020, **195**, 109073.
23 (*a*) R. Blume, D. Rosenthal, J. P. Tessonnier, H. Li, A. Knop-Gericke and R. Schlögl, *ChemCatChem*, 2015, **7**, 2871; (*b*) T. R. Gengenbach, G. H. Major, M. R. Linford and C. D. Easton, *J. Vac. Sci. Technol., A*, 2021, **39**, 013204.
24 (*a*) A. C. Ferrari, *Solid State Commun.*, 2007, **143**, 47; (*b*) A. C. Ferrari and D. M. Basko, *Nat. Nanotechnol.*, 2013, **8**, 235.
25 A. García-Miranda Ferrari, C. W. Foster, P. J. Kelly, D. A. Brownson and C. E. Banks, *Biosensors*, 2018, **8**, 53.
26 (*a*) T. Han, S. Kundu, A. Nag and Y. Xu, *Sensors*, 2019, **19**, 1706; (*b*) A. Kalkal, P. Allawadhi, P. Kumar, A. Sehgal, A. Verma, K. Pawar, R. Pradhan, B. Paital and G. Packirisamy, *Sens. Int.*, 2022, 100180.
27 (*a*) F. M. de Oliveira, E. I. de Melo and R. A. da Silva, *Sens. Actuators, B*, 2020, **321**, 128528; (*b*) B. C. Janegitz, R. D. Crapnell, P. Roberto de Oliveira, C. Kalinke, M. J. Whittingham, A. Garcia-Miranda Ferrari and C. E. Banks, *ACS Meas. Sci. Au*, 2023, **3**(3), 217.